

Computer Modeling & Simulation

Minimizing Air Entrainment in a Shot Sleeve during Slow-Shot Stage

Michael R. Barkhudarov, Vice President of Research & Development
Flow Science Inc.
 Santa Fe, New Mexico

Introduction

The speed of the plunger in a horizontal shot sleeve must be carefully controlled to avoid unnecessary entrainment of air in the metal and, at the same time, minimize heat losses in the sleeve. If the plunger moves too fast, large waves are created on the surface of the liquid metal that may overturn and entrain air into the metal, which will then be carried into the die cavity. A plunger moving too slowly results in waves reflecting from the opposite end of the shot sleeve. The reflected waves prevent proper expulsion of air into the die cavity. In either case, the outcome is excessive porosity in the final casting.

In this article, a general solution is derived for the plunger speed as a function of time that allows the engineers to precisely control the behavior of metal in the shot sleeve during the slow-shot stage of the high pressure filling process, minimizing the risk of air entrainment. The results are validated using a full-physics, 3-D CFD analysis [FLOW-3D®, 2009].

Mathematical Model

The dynamics of waves in a horizontal shot sleeve can be analyzed by drawing an analogy with flow in an open channel. From the start, a cylindrical shot sleeve is approximated with a channel of rectangular cross-section filled initially with liquid metal to the depth h_0 . This simplification of the shape of the cylinder is justified for initial fill fractions in the range of 40-60% [Lopez *et al*, 2003] and allows for some useful solutions. For a shallow wave travelling along the free surface due to gravity g , the speed of the wave, c_0 , is given by

$$c_0 = \sqrt{gb_0} \quad (1)$$

This equation is valid for waves that are long and shallow compared to the mean depth of the fluid (Figure 1, top). Note that the wave speed is independent of the properties of the metal. If the speed of the plunger is too slow, these waves will travel a combined distance equal

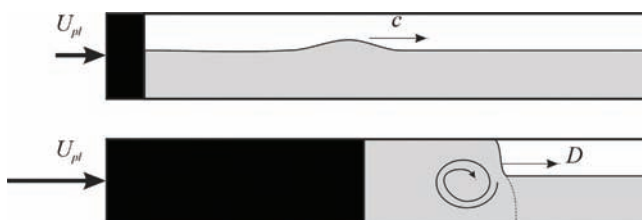


Figure 1 – Schematic illustration of the propagating surface wave when the plunger is moving slowly (top) and the hydraulic jump forming ahead of the fast moving plunger.

to several times the length of the sleeve, reflecting off the moving plunger and the opposite end of the sleeve, before a transition to the fast shot takes place.

As the plunger accelerates, it first catches up, then overtakes the waves; that is, the flow becomes *super-critical*. As a result, metal piles up to the top of the sleeve in front of the plunger, creating a flow condition called *hydraulic jump*, at which the flow undergoes a sharp transition from a relatively slow and laminar regime downstream to a fast and turbulent one behind the jump. Figure 1, bottom, schematically illustrates the two flow zones in a short sleeve separated by a hydraulic jump.

If the relatively slow speed of the metal in front of the jump is neglected, then the speed of this front, D , can be estimated from the balance of mass as

$$D = \frac{U_p}{1 - \varepsilon} \quad (2)$$

where U_p is the plunger velocity and ε is the fill fraction of the sleeve ahead of the front [Garber, 1982]. Equation 2 shows that the hydraulic jump always moves faster than the plunger and that, just like for the wave speed in Equation 1, its speed is independent of the metal properties.

Equations 1 & 2 provide some guidance to what the plunger speed can be during the slow-shot stage. A more detailed analysis is possible by modeling the flow of metal in a rectangular shot sleeve of length L and height H using the shallow water approximation [Lopes *et al*, 2000]. In this approximation, the flow in the vertical direction is neglected in comparison with the horizontal velocity component. The flow is modeled in two dimensions, with the x axis directed along the direction of motion of the plunger, and the z axis pointing upwards. If viscous forces are omitted, then the flow has only one velocity component, u , along the length of the channel. Pressure at every point in the flow is then hydrostatic

$$P = P_0 + \rho g(b - z) \quad (3)$$

where $b(x, t)$ is the height of the fluid at point x and time t , as shown in Figure 2.

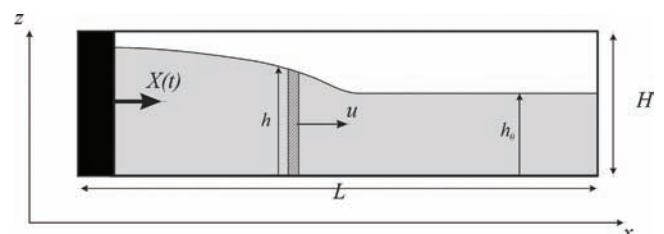


Figure 2 – Schematic representation of the flow in a shot sleeve and the coordinate system.

With these assumptions, the equations governing the evolution of the flow velocity u are

$$\frac{\partial(u+2c)}{\partial t} + (u+c) \frac{\partial(u+2c)}{\partial x} = 0 \quad (4)$$

$$\frac{\partial(u-2c)}{\partial t} + (u-c) \frac{\partial(u-2c)}{\partial x} = 0$$

Where

$$c(x, t) = \sqrt{gb} \quad (5)$$

The plunger speed in the positive x direction is given by $dX/dt=X'(t)$, where $X(t)$ defines the position of the plunger at time $t>0$. At the moving surface of the plunger $u(X(t), t) = X'(t)$.

Equation 4 defines two sets of waves traveling at the respective speeds of $u+c$ and $u-c$ along the metal surface. As the plunger moves along the length of the channel, it sends waves traveling forward along the metal surface. Each wave is associated with a small segment of the metal's free surface and the column of metal directly below it (Figure 2). The metal location, speed and depth in a wave that separates from the surface of the plunger at time $t=t_p$ are given by [Lopes *et al*, 2000]:

$$x(t) = X(t_p) + \left(c_0 + \frac{3}{2} X'(t_p)\right) \cdot (t - t_p)$$

$$u(x, t) = X'(t_p) \quad (6)$$

$$h(x, t) = \frac{1}{g} \left(\sqrt{gb_0} + \frac{1}{2} X'(t_p) \right)^2$$

Plunger Acceleration

According to Equation 6, the metal speed, u , and depth, h , in each wave are constant and depend only on the time of the wave separation from the plunger, t_p . They both increase with the speed of the plunger X' . Therefore, the first conclusion is that to maintain a monotonic slope of the metal surface in the direction away from the plunger, the latter *must not decelerate*, that is:

$$X''(t) \geq 0 \quad (7)$$

If this condition is not satisfied, then there will be waves sloped in both directions, as shown in Figure 1, top. When they reflect off the end of the sleeve and travel back towards the plunger, it creates unfavorable conditions for the evacuation of air from the sleeve and into the die cavity.

Controlling the Waves

Once a wave detaches from the plunger, it travels at a constant speed given by

$$u+c = X'(t_p) + \sqrt{gb} = \sqrt{gb_0} + \frac{3}{2} X'(t_p) \quad (8)$$

If the plunger accelerates, then each successive wave will move faster than the waves generated earlier. This will lead to a steepening of the surface slope as the waves travel further down the channel and can potentially result in overturning. If the speed of the plunger can be controlled as to limit the wave steepening during the slow-shot stage, then the overturning can be avoided.

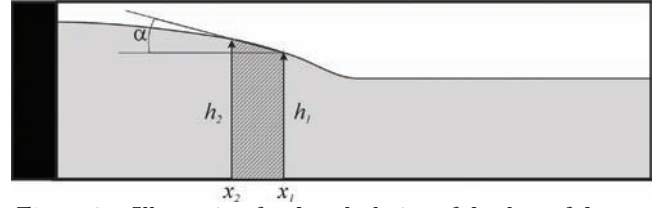


Figure 3 – Illustration for the calculation of the slope of the metal's free surface.

Let us analyze the evolution of the surface slope between two waves generated at the plunger at close instances, $t_2 > t_1$ (Figure 3) [Reikher and Barkhudarov, 2007]. The slope is given by

$$\tan(\alpha) = -\frac{dh}{dx} = -\frac{h_1 - h_2}{x_1 - x_2} \quad (9)$$

Using expression for x and h in Equation 6, the right-hand side can be rewritten as

$$\tan(\alpha) = \frac{\left(c_0 + \frac{1}{2} X'(t_1)\right)^2 - \left(c_0 + \frac{1}{2} X'(t_2)\right)^2}{g \left[X(t_1) - X(t_2) + \left(c_0 + \frac{3}{2} X'(t_1)\right)(t - t_1) - \left(c_0 + \frac{3}{2} X'(t_2)\right)(t - t_2) \right]} \quad (10)$$

After linearizing the right-hand side with respect to $\Delta t = t_2 - t_1$, the equation is obtained for the wave slope as a function of the plunger speed at the time of the wave creation, $t=t_p$, and time t :

$$\tan(\alpha) = \frac{1}{g} \cdot \frac{\left(c_0 + \frac{1}{2} X'(t_1)\right) \cdot X''(t_1)}{c_0 + \frac{1}{2} X'(t_1) - \frac{3}{2} X''(t_1) \cdot (t - t_1)} \quad (11)$$

Interestingly, if the plunger moves at a constant speed, *i.e.* $X''(t_p)=0$, then the right-hand side of Equation 11 becomes zero and the slope of the free surface horizontal.

If the plunger accelerates, then the denominator on the right-hand side of Equation 11 decreases, and the slope increases with time. When the denominator reaches zero, the slope becomes vertical. The maximum slope in a wave, α_{max} is achieved when the wave reaches the end of the shot sleeve at $t=t_L$. This time can be computed from the constant wave speed and the distance it has to travel from the point of its creation at the plunger surface to the end of the sleeve at $x=L$:

$$t_L = t_1 + \frac{L - X(t_1)}{c_0 + \frac{3}{2} X'(t_1)} \quad (12)$$

Replacing t in Equation 11 with t_L and rearranging terms yields

$$X''_{\alpha_{max}}(t_1) = \frac{\left(c_0 + \frac{1}{2} X'(t_1)\right) \cdot \left(c_0 + \frac{3}{2} X'(t_1)\right) \cdot \tan(\alpha_{max})}{\frac{1}{g} \cdot \left(c_0 + \frac{1}{2} X'(t_1)\right) \left(c_0 + \frac{3}{2} X'(t_1)\right) + \tan(\alpha_{max}) \cdot (L - X(t_1))} \quad (13)$$

Equation 13 can now be used to calculate the velocity of the plunger as a function of time that maintains a *certain* slope of the metal surface during the slow-shot stage. For example, if α_{max} is set equal to 10° , then the plunger accelera-

tion given by Equation 13 ensures that the slope of 10° is not exceeded *anywhere* and *anytime* during the motion of the plunger. Note that the plunger velocity given by Equation 13 is only a function of the initial amount of metal, h_0 , and the length of the sleeve, L , and not of the metal properties.

Equation 13 can be used to obtain the slope α_{min} of the metal surface right at the plunger by setting $t=t_1$:

$$\tan(\alpha_{min}) = \frac{X''(t_1)}{g} \quad (14)$$

Equation 14 gives the *initial* surface slope for a wave detaching from the plunger at time $t=t_1$; it is a function of only the plunger's acceleration and not its position or even velocity. As the wave propagates along the length of the channel, it steepens, reaching the maximum slope, α_{max} , at the end of the channel at $x=L$, given by Equation 13.

Equations 7 and 13 give a range of values for the plunger acceleration at any give time

$$0 \leq X''(t) \leq X''_{\alpha_{max}}(t) \quad (15)$$

Two things are achieved when the plunger acceleration stays within this range. First, the slope of the metal surface is directed away from the plunger and towards the opposite end of the shot cylinder, helping to direct the air from the sleeve and into the runner system. Secondly, the slope will not exceed the angle defined by α_{max} at any time during the slow-shot process, preventing wave overturning and the entrainment of air in the metal.

Results

Equation 13 is an ordinary differential equation (ODE) that can be easily integrated numerically to obtain the solutions for $X(t)$ and $X'(t)$. The integration is done with respect to t_1 , using the initial values of the plunger location and speed at $t=0$: $X(0)=0$ and $X'(0)=0$.

Figure 4 shows numerical solutions for the plunger position, $X(t)$, acceleration, $X''(t)$, and speed, $X'(t)$, (the latter is shown as a function of both time and distance along the channel length) for several values of α_{max} . The integration was done for a shot cylinder of length $L=0.7$ m and height of $H=0.1$ m and the initial fill fraction of 40%, i.e., $h_0=0.04$ m.

As expected, the plunger motion is slower for smaller values of α_{max} . It takes the plunger 1.66 seconds to get to the end of the shot sleeve for the most conservative case considered with $\alpha_{max}=5^\circ$, while for $\alpha_{max}=90^\circ$, the time is 0.83 seconds. However, these times will be longer if there is an additional constraint of the plunger velocity not to exceed the *critical velocity* at which the metal surface reaches the ceiling of the channel at $h=H$ [Garber, 1982]. The critical velocity of the plunger can be derived from the solution for the metal depth $h(t,x)$ given by Equation 6 [Tszeng and Chu, 1994]:

$$X'_{cr} = 2(\sqrt{gH} - \sqrt{gh_0}) \quad (16)$$

and is shown in Figure 4 by the horizontal dashed line. For the selected parameters of the shot sleeve, $X'_{cr}=0.73$ m/sec. Even for $\alpha_{max}=5^\circ$, the plunger velocity reaches the critical value after it moved just over 60% of the channel length, at $t_c=1.35$ sec. For steeper surface slopes, the critical velocity is reached at earlier times, for example, for $\alpha_{max}=90^\circ$ $t_c=0.58$ sec and the plunger position is 22% of L .

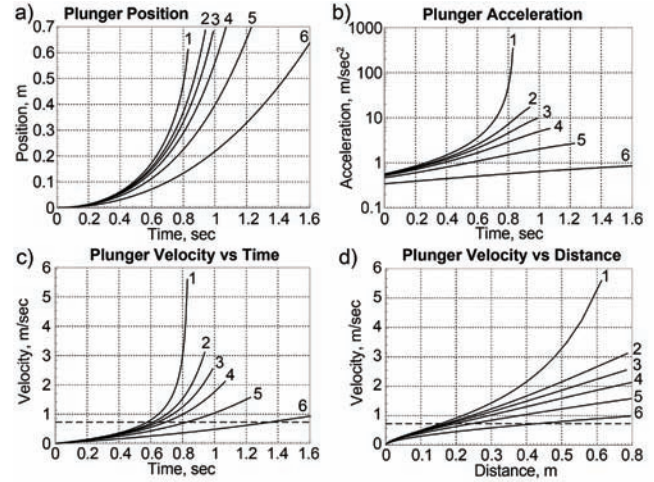


Figure 4 – Solutions of Equation 13 for a) the plunger position, b) acceleration, c) velocity and d) velocity as a function of distance along the length of the shot channel (d), at different maximum surface slopes α_{max} : 1 – 90° , 2 – 60° , 3 – 45° , 4 – 30° , 5 – 15° and 6 – 5° . The horizontal dashed lines on plots c and d represent the critical plunger velocity.

When the plunger reaches the critical velocity, the metal surface comes in contact with the ceiling of the shot cylinder. Beyond this point, the shallow water theory used here becomes invalid. It can also be argued that if the plunger continues to accelerate, then the potential for creating an overturning wave increases since all the energy of the flow is now redirected forward by the walls and ceiling of the channel. It is usually recommended to limit the plunger velocity to the critical value during the slow-shot stage.

Validation

Three-dimensional simulations that include all the important physics of the die casting process remain, of course, the best way to validate the designs [Reikher, Barkhudarov, 2007, Nikroo *et al*, 2009]. Simulation was used to validate some of the predictions of the simplified model. In the simulation, more realistic conditions of viscous flow and a circular channel cross-section are used. Heat transfer and solidification are not included in the model, based on the assumption that solidification in the shot sleeve is minimal, if any, and does not significantly affect the flow.

The length of the channel is $L=0.7$ m, the same as the one used to obtain solutions in Figure 4. The shot diameter

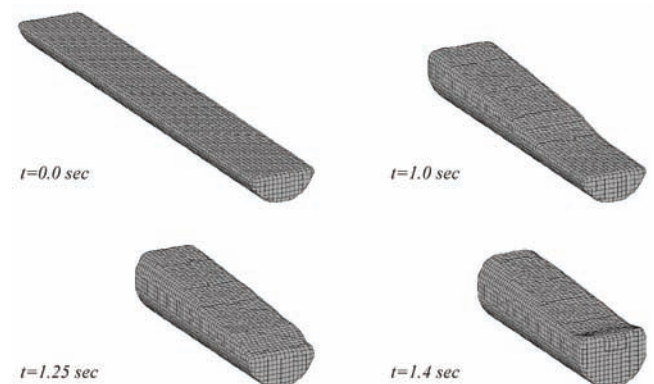


Figure 5 – Three-dimensional snapshots of the metal in the shot cylinder during the slow-shot stage.

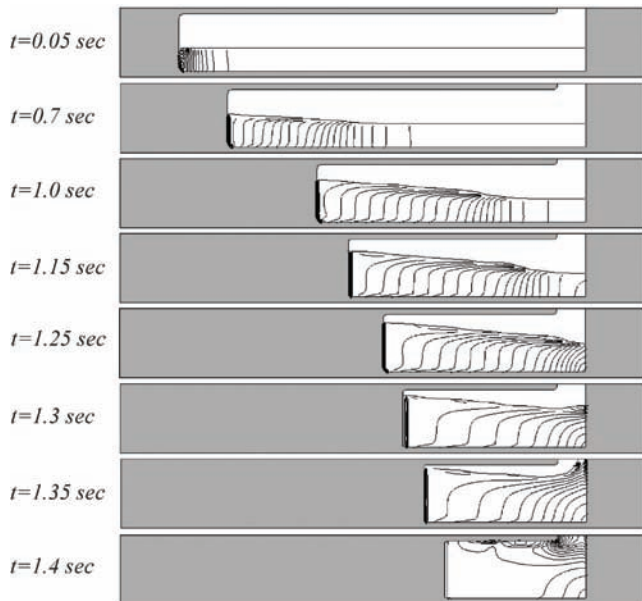


Figure 6 – Two-dimensional snapshots of the metal in the shot cylinder, shown in the vertical symmetry plane, during the slow-shot stage. Contour lines indicate the variation of the horizontal velocity magnitude.

is $D=0.1$ m, and the initial fluid depth is $h_0=0.04$ m. The velocity of the plunger is defined as a function of time using the solution for the maximum slope of the metal surface of $\alpha_{max}=5^\circ$, given by Equation 13 (Curve 6 in Figure 4c). Two- and three-dimensional results are shown in Figures 5 and 6.

There are several aspects of the numerical solution that match the analytical solution quite well. The slope of the wave largely stays within the 5° limit. The circular nature of the channel does not seem to affect much the profile of the free surface in the transverse direction. The critical point, at which the metal surfaces touches the top of the channel, is reached at $t=1.37$ sec, very close to where Curve 6 crosses with the critical velocity on Figure 4c. The velocity of the plunger at that time is 0.725 m/sec, close to the value of 0.73 m/sec given by Equation 16 for the rectangular channel. Finally, the first wave arrives at the end of the shot sleeve at $t=1.15$ sec, while the theory predicts 1.12 sec, based on the wave speed in the undisturbed flow given by Equation 1.

Given the 3-D nature of the simulation and the fact that the flow is viscous, the agreement with the analytical solution is quiet remarkable. Note that the same initial depth of metal, h_0 , was used for the round shot sleeve in the simulation and for the rectangular one in the analytical solution. In the present example, with $h_0=0.04$ m, the initial fill fraction in the circular cylinder comes to 37.4%, as opposed to 40% for the rectangular channel. If the same initial fill fraction was used instead, the results of the two solutions would not be so close.

This is not saying that no differences exist in the two solutions. The velocity contours shown in the plane of symmetry in Figure 6 indicate that one of the main assumptions used to obtain the analytical solution — that all flow variables vary only along the horizontal direction — does not quite hold. First, a viscous boundary layer develops at the bottom of the shot sleeve. Secondly, the numerical results show that flow near the free surface moves faster than the bulk of the metal below it, resulting in a sort of a surge wave. The slope of the metal surface in this wave is about one-and-a-half to two times larger than 5° . It reaches the end of the channel at

around 1.3 sec and then reflects back. As a result, air may be entrained in the last stages of the process unless, for example, the reflected surge wave is redirected into the runner system.

Conclusions

It is often assumed that the overturning of the metal surface that causes air entrainment occurs when the wave profile becomes vertical, that is $\alpha_{max}=90^\circ$. In reality, the breaking of the wave surface may happen at more moderate angles, as can be seen while observing ocean waves. Equation 13 allows the engineers to define any maximum permitted wave slope, obtaining a sufficient safety margin to avoid any air entrainment.

Being able to define a safety margin for the surface slope is also important because some simplifications were made in arriving at the solution, such as replacing the cylindrical channel with a rectangular one. Obviously, the curved walls of the shot cylinder will exacerbate the potential for wave overturning as the metal level rises. Besides, the critical velocity is attained faster in a cylindrical channel than in a rectangular one of the same width; therefore, an extra safety margin must be used in the estimation of the critical velocity.

The requirement of minimum air entrainment must, of course, be combined with other criteria that control the quality of the casting, like a specific filling rate and minimal heat losses in the shot sleeve and the runner system.

About the Author

Michael Barkhudarov graduated from Moscow State University in 1985 with a M.Sc. in mechanical engineering. He earned his doctorate in mechanical engineering from The University of Sheffield in 1995. He has been working at Flow Science Inc. since 1994 and currently is the vice president of R&D.

References

1. Garber L.W. Theoretical Analysis and Experimental Observation of Air Entrapment During Cold Chamber Filling. *Die Casting Engineer*, May/June 1982.
2. Lopez J., Faura F., Hernandez J., Gomez P. On the Critical Plunger Speed and Three-Dimensional Effects in High-Pressure Die Casting Injection Chambers. *Manufacturing Science*. 125, 529 – 537, August 2003.
3. Lopez J., Hernandez J., Faura F., Trapaga G. Shot Sleeve Wave Dynamics in the Slow Phase of Die Casting Injection. *ASME, Fluid Engineering* 122, 349 – 356, June 2000.
4. Reikher A., Barkhudarov, M.R. *Casting: An Analytical Approach*, Springer-Verlag, London, 2007.
5. Tszeng T.C., Chu Y.L. A Study of Wave Formation in Shot Sleeve of a Die Casting Machine. *ASME, Eng.* 116, 175 – 182, May 1994.
6. Nikroo A.J., Akhlaghi M., Najafabadi, M.A. Simulation and Analysis of Flow in the Injection Chamber of Die Casting Machine During the Slow Shot Phase. *International Journal of Advanced Manufacturing Technology*, 41, 31-41, 2009.
7. FLOW-3D®, Flow Science, Inc., Santa Fe, USA, <http://www.flow3d.com>, 2009.